IL NUOVO CIMENTO **45 C** (2022) 67
DOI 10.1393/ncc/i2022-22067-x

COMMUNICATIONS: SIF Congress 2021

The MUonE experiment

R. N. PILATO([1])([2])

([1]) *INFN, Sezione di Pisa - Pisa, Italy*
([2]) *Dipartimento di Fisica, Università di Pisa - Pisa, Italy*

received 30 January 2022

Summary. — The latest measurement of the muon g-2, performed by the Muon g-2 Collaboration at Fermilab, presently exhibits a 4.2σ discrepancy from the Standard Model prediction. The hadronic contribution a_μ^{HLO} represents the main source of uncertainty on the theoretical prediction. The MUonE experiment proposes a novel approach to determine a_μ^{HLO} by measuring the running of the electromagnetic coupling constant in the space-like region, via $\mu - e$ elastic scattering. The measurement will be performed by scattering a 160 GeV muon beam, currently available at CERN's North Area, on the atomic electrons of a low-Z target. A Test Run on a reduced detector is planned to validate this proposal. The status of the experiment in view of the Test Run will be presented.

1. – Introduction

The muon magnetic anomaly is defined as $a_\mu = (g_\mu - 2)/2$, where g_μ is the gyromagnetic ratio. It is a low energy observable which can be both computed and measured with very high precision, and can be used as a stringent test of the Standard Model. Recently, the E989 Muon g-2 Collaboration at Fermilab announced its first result for a_μ [1], which is in excellent agreement with the previous measurement performed by the BNL E821 experiment [2]. The combination of the two experimental values leads to a 4.2σ discrepancy with the Standard Model prediction recommended by the Muon g-2 Theory Initiative [3]. The corresponding scenario is represented in fig. 1.

In the next years, the accuracy on a_μ will be further improved by the E989 experiment, which aims to reach the remarkable accuracy of 0.14 ppm [4]. Moreover, a new technique will be exploited at J-PARC to measure a_μ in an independent way [5]. Consequently, an improvement is also required on the theoretical prediction, as its uncertainty will become the main limitation for a test of the Standard Model.

The accuracy on the Standard Model calculation is limited by the evaluation of the leading order hadronic contribution a_μ^{HLO}, which takes into account for one loop quark vacuum polarization insertions in the electromagnetic current of the muon magnetic

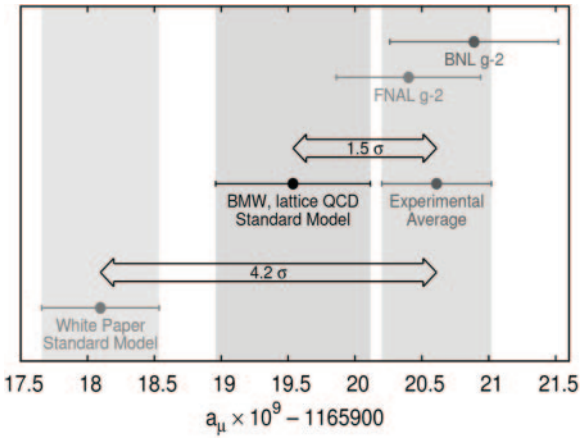

Fig. 1. – From the top to the bottom: experimental values of a_μ measured by BNL E821 [2], Fermilab E989 [1] and their combined average. Standard Model evaluation of BMW Collaboration using lattice QCD [7] is also shown, as well as the value recommended by the Muon g-2 Theory Initiative [3].

anomaly lowest order diagram [6]. The reason for that lies in the calculation involving strong interactions at low energies, for which the perturbative approach cannot be employed. Therefore, a_μ^{HLO} is traditionally determined by means of a dispersion integral on the annihilation cross section $e^+e^- \to$ hadrons. However, such a cross section is densely populated by resonances and influenced by flavour threshold effects, which limit the final precision achievable by this method. Despite these difficulties, the calculation of a_μ^{HLO} reached an accuracy of $\sim$0.6% [3].

In addition to this, a recent evaluation of a_μ^{HLO} based on lattice QCD calculation reached for the first time an accuracy comparable to the dispersive approach [7]. Nevertheless, there is a tension of 2.2σ between these two theoretical evaluations, and the lattice QCD value weakens the discrepancy between theory and experiment to 1.5σ, as shown in fig. 1. An independent crosscheck of a_μ^{HLO} is therefore required to solve this tension and consolidate the theoretical prediction.

MUonE proposes an innovative method to measure a_μ^{HLO}. It is based on the direct measurement of the hadronic contribution to the running of the electromagnetic coupling constant ($\Delta\alpha_{had}$) in the space-like region [8]. The following equation will be used to calculate a_μ^{HLO} [9]:

$$a_\mu^{HLO} = \frac{\alpha}{\pi} \int_0^1 \mathrm{d}x (1-x) \Delta\alpha_{had}[t(x)]. \tag{1}$$

Here, α is the fine structure constant, and the integration variable x is related to the space-like momentum transfer t through the formula

$$t(x) = \frac{x^2 m_\mu^2}{x-1} < 0, \tag{2}$$

where m_μ is the muon mass.

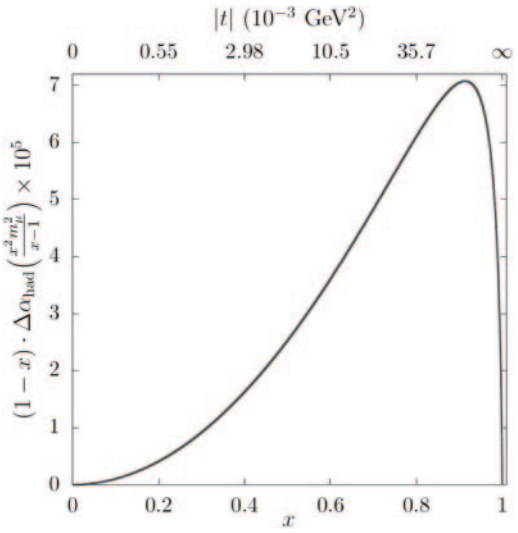

Fig. 2. – Integrand $(1-x)\Delta\alpha_{had}[t(x)] \times 10^5$ as a function of x or t (upper scale) [10].

Figure 2 shows the integrand function of the master integral in eq. (1). The peak of the integrand occurs at $x_{peak} \simeq 0.914$, which corresponds to a momentum transfer $t_{peak} \simeq$-0.108 GeV^2. Here, $\Delta\alpha_{had}(t_{peak}) \simeq 7.86 \times 10^{-4}$.

The main advantage of this method is that $\Delta\alpha_{had}$ is a smooth function for negative momentum transfer, in contrast with the time-like e^+e^- data used in the traditional dispersive approach. A further advantage is that the electromagnetic running in the region of interest for the evaluation of a_μ^{HLO} can be measured by a single scattering experiment. For this reason, the space-like approach is not affected by the systematic uncertainties due to handling data from different experiments, which instead are relevant for the time-like dispersive method. Therefore, the method proposed by MUonE allows a completely independent estimation of a_μ^{HLO}, which can be compared with time-like and lattice QCD results towards a firmer prediction of a_μ.

2. – The MUonE experimental proposal

The MUonE experiment aims to extract $\Delta\alpha_{had}(t)$ from a precise measurement of the shape of the differential cross section of the $\mu^+e^- \to \mu^+e^-$ elastic scattering [10]. The measurement is performed by scattering a high energy muon beam on the atomic electrons of a low-Z target. A 160 GeV muon beam, currently available at CERN M2 beamline, allows to cover the momentum transfer region $-0.153\,\text{GeV}^2 < t < 0\,\text{GeV}^2$, which is equivalent to $0 < x < 0.936$. This corresponds to ∼87% of the master integral in eq. (1). The remaining fraction can be computed by extrapolating $\Delta\alpha_{had}(t)$ with an appropriate parameterization [11].

An attractive feature of the $\mu - e$ elastic process lies in its simple kinematics, which makes the scattering angles of the outgoing electron and muon correlated. This constraint allows to select elastic events and reject background, which is expected to be mainly due to e^+e^- pair production by muons in the target. Moreover, kinematics is highly boosted in the forward direction in the laboratory frame, due to the high energy muon beam

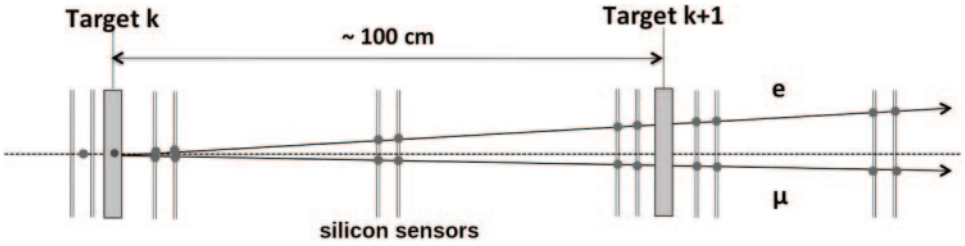

Fig. 3. – Sketch of a single station (image not to scale).

employed. This allows using a single detector to cover the full acceptance, since the elastic events which are interesting for the experiment are contained within ∼32 mrad for the electron and within ∼5 mrad for the muon.

The experimental apparatus consists of a repetition of 40 identical stations. A sketch of a single station is shown in fig. 3. It is composed of a ∼15 mm thick target, followed by a tracking system with a lever arm of ∼1 m, which consists of 3 pairs of Silicon strip detectors with orthogonal strips and is used to measure the scattering angles with high precision. An electromagnetic calorimeter is placed downstream of all the stations, in order to provide e/μ particle identification in the low angles region. The apparatus will also be equipped with a muon filter, placed downstream of the calorimeter.

The modular structure of MUonE allows re-using the incoming muon beam for each station, which acts as an independent unit. In this way, $\mu - e$ elastic events will be distributed along the entire apparatus, increasing the collected statistics but minimizing the thickness of a single target at the same time. This helps to keep multiple scattering effects under control, which break the $\mu - e$ angular correlation. For this purpose, a low-Z material as Beryllium or Carbon will be used for the target.

Given the total target thickness of 60 cm and the average intensity of $\sim 1.3 \times 10^7$ μ/s of the CERN M2 beamline, MUonE can reach an integrated luminosity of about 1.5×10^7 nb^{-1} in 3 years of data taking. This is equivalent to collecting $\sim 4 \times 10^{12}$ elastic events with electron energy >1 GeV, and allows achieving a statistical error of ∼0.3% on a_μ^{HLO}. This makes the measurement of MUonE competitive with the time-like evaluation.

The main challenge of the experiment is to keep the systematic error at the same level as the statistical one. This is equivalent to measuring the shape of the differential cross section with a systematic accuracy of O(10 ppm) at the peak of the integrand function [10]. Such an accuracy can be achieved only with a twofold effort, both on the theoretical and experimental side. From the experimental point of view, the most relevant sources of systematic uncertainties are the longitudinal alignment of a station, which must be controlled at the level of 10 μm, the knowledge of the average beam energy, which needs to be determined with a precision of few MeV [11], and multiple scattering effects. Preliminary analyses indicate that these effects can be controlled at the required values. Results from a Test Beam performed at CERN with 12–20 GeV electrons on 8–20 mm Carbon targets show a satisfactory agreement between data and GEANT4 simulation [12].

On the theoretical side, the development of high precision Monte Carlo tools is needed, since the radiative corrections to the differential cross section must be included up to the NNLO to meet the requirement of O(10 ppm) systematic uncertainty. Presently, the full set of NLO QED and electroweak corrections is completed, and a fully exclusive Monte Carlo generator is available [13]. The NNLO hadronic corrections have been computed in [14,15], while the two-loop integrals relevant for the NNLO QED corrections have been

evaluated in [16-18]. Very recently, the analytic evaluation of the two-loop corrections to the process $e^+e^- \to \mu^+\mu^-$ has been completed [19] treating the electron as a massless particle and the muon as a massive particle.

Moreover, the exact NNLO photonic corrections on the leptonic legs, including all mass terms, have been implemented in two independent fully exclusive Monte Carlo codes [20, 21]. Results from these codes are in very good agreement. Furthermore, the complete NNLO corrections including a lepton pair have been calculated and implemented in a Monte Carlo code [22]. Resummation of leading terms in higher orders matched to NNLO is necessary and is being carried out. Work is also in progress to interface the Monte Carlo generator with the GEANT4 detector simulation. In addition to this, the massive three-loop vector form factors have been computed recently in [23]. This represents a first step to improve the theoretical precision up to NNNLO.

Very recently, exact analytic expressions have been presented to compute also the hadronic vacuum polarization contribution to the muon g-2 in the space-like region at NLO (a_μ^{HNLO}) [24]. This will allow MUonE to extend its determination of the hadronic contribution to a_μ, also including the NLO.

Reference [25] gives a state-of-the-art review of the theoretical progress in MUonE. Possible new physics effects in $\mu - e$ elastic scattering have been investigated in [26, 27], and are expected to lie below MUonE sensitivity.

3. – Test run

A Letter of Intent has been submitted to the CERN SPS Committee in 2019 [11], obtaining recommendations for a Test Run of 3 weeks to validate the experimental proposal. Initially, it was foreseen for Fall 2021, but it will be rescheduled because of Covid-19 and delays in the procurement of tracker components. A parasitic run with four Silicon detectors was performed at the M2 beamline from 25th October to 15th November 2021, and provided a first proof of concept of the MUonE readout chain.

The Test Run detector will be composed of two full MUonE stations followed by an electromagnetic calorimeter. A further tracking station without target will be placed upstream of the apparatus, to detect the incoming muons.

The basic tracking unit has been chosen to be the 2S modules developed for the CMS Outer Tracker upgrade [28]. Figure 4 shows a schematic view of a 2S module. Each module is composed of 2 Silicon strip sensors separated by 1.8 mm, with the same

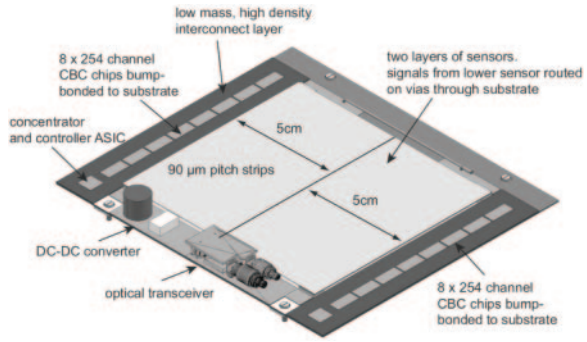

Fig. 4. – Schematic representation of a 2S module [11].

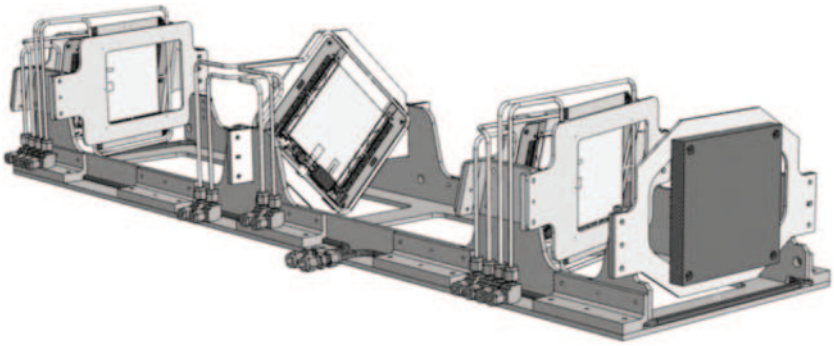

Fig. 5. – CAD drawing of a MUonE station.

dimension and strip orientation, thus reading the same coordinate. Each sensor is 320 μm thick, with an area of approximately $10 \times 10\,\mathrm{cm}^2$. Therefore, a single module allows covering the full angular acceptance, ensuring a uniform response over all the scattering angles. The two sensors composing a module are mounted on the same mechanical structure, and are read out by the same front-end electronics, which compares signals from the two sensors to find correlated hits. This feature can be exploited to reject large angle tracks and suppress background from single sensor hits. The read-out rate at 40 MHz is capable of sustaining the M2 beamline in-spill rate (50 MHz), thus minimizing the pileup. 2S modules have a single hit resolution of $\sim 20\,\mu$m, which can be further improved by tilting the module around an axis parallel to the strip orientation of its sensors. Simulation studies show that a tilt of 233 mrad ($\sim 14^\circ$) improves the single hit resolution to $\sim 10\,\mu$m, keeping a high detection efficiency at the same time.

The current setup of a MUonE station is represented in fig. 5. 2S modules in the first and third pairs are tilted to implement the single hit resolution improvement, while the second pair is rotated by 45° around the beam axis in order to solve reconstruction ambiguities, and its modules are not tilted. The mechanical structure is made of Invar. It is a Fe-Ni alloy which has a low coefficient of thermal expansion ($\sim 1.2 \times 10^{-6}\,\mathrm{K}^{-1}$), in order to meet the stringent request of 10 μm on the stability of the longitudinal size. For this purpose, an enclosure and a cooling system have also been designed to keep the temperature of the station constant within 1 °C.

Presently, an aluminum mockup has been manufactured to test the mechanical structure planarity and the correct integration of the 2S modules. Stepper motors are used to align the station with the muon beam.

The electromagnetic calorimeter to be used in the Test Run is composed of a matrix of 5×5 $PbWO_4$ crystals. The total area of $14 \times 14\,\mathrm{cm}^2$ allows covering the full acceptance for the scattering events from the two MUonE stations. Each crystal has a section of $2.85 \times 2.85\,\mathrm{cm}^2$ and a length of 22 cm ($\sim 25 X_0$), and will be read-out by APD sensors. Tests on sensors and crystal response are currently ongoing.

The Test Run will be mainly aimed at monitoring the mechanical and thermal stability of the apparatus, as well as confirming the validity of the system engineering. It will be crucial to test the alignment procedures and check the front-end electronics and the DAQ system. The main difference between CMS operations at LHC and MUonE is that the signals from the M2 muon beam will be asynchronous with respect to the 2S modules clock. Therefore, an appropriate configuration of the front-end electronics must be adopted to manage this aspect. It has been preliminarily tested during the last

parasitic run, and will be optimized in the Test Run.

Data streams from the 2S modules and the calorimeter will be processed by a single Serenity board [29]. No event selection will be applied during the Test Run. All the information will then be used to elaborate online selection algorithms to be implemented in the Full Run with 40 stations.

Assuming to accomplish these primary goals in the first two weeks of running, the remaining days could be exploited to collect $\sim 5\,\mathrm{pb}^{-1}$ of good quality data, corresponding to $\sim 10^9$ elastic events with electron energy $>1\,\mathrm{GeV}$. Such a data sample will allow measuring the leptonic contribution to the electromagnetic running, which is $\lesssim 10^{-2}$ in our kinematic range. Moreover, it could be enough to get an initial sensitivity to $\Delta\alpha_{had}(t)$, which is $\lesssim 10^{-3}$ in the MUonE kinematic region.

The effect of $\Delta\alpha_{had}(t)$ on the shape of the differential cross section can be displayed considering the ratio R_{had} between the observed differential cross section and the theoretical prediction computed assuming only the presence of the leptonic running. It turns out to be [11]

$$R_{had} \sim 1 + 2\Delta\alpha_{had}(t). \tag{3}$$

Figure 6 shows the expectation of R_{had} as a function of the muon scattering angle, obtained using the MUonE NLO Monte Carlo generator and a fast simulation including the detector intrinsic resolution and multiple scattering effects. The extraction of $\Delta\alpha_{had}(t)$ is carried out by means of a template fit method [11]. The hadronic running is modeled using the following parameterization [11]:

$$\Delta\alpha_{had}(t) = KM\left\{-\frac{5}{9} - \frac{4}{3}\frac{M}{t} + \left(\frac{4}{3}\frac{M^2}{t^2} + \frac{M}{3t} - \frac{1}{6}\right)\frac{2}{\sqrt{1-\frac{4M}{t}}}\ln\left|\frac{1-\sqrt{1-\frac{4M}{t}}}{1+\sqrt{1-\frac{4M}{t}}}\right|\right\}. \tag{4}$$

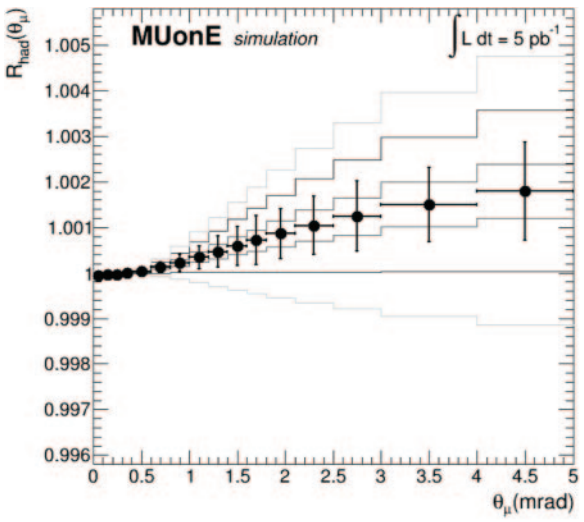

Fig. 6. – Ratio R_{had} as a function of the muon scattering angle. The error bars correspond to the statistical uncertainties for an integrated luminosity of $5\,\mathrm{pb}^{-1}$. Lines without errors represent templates for different values of the parameter K in eq. (5).

This ansatz adopts the functional form of the pure QED leading order contribution to the electromagnetic running induced by a lepton pair in the space-like region. In the leptonic case, M is the squared lepton mass, while $k = KM = \alpha/\pi$. On the contrary, these parameters do not have any precise physics interpretation for the hadronic running, since $\Delta\alpha_{had}$ is not calculable in perturbation theory. Equation (4) was preliminarly tested against a numerical parameterization of $\Delta\alpha_{had}$, and the level of agreement is excellent [11]. In the limit of small $|t|$, eq. (4) behaves like

$$\Delta\alpha_{had}(t) \simeq -\frac{1}{15}Kt \tag{5}$$

This is the dominant behaviour in the MUonE kinematic region [11]. Therefore, given the limited statistics which will be collected in the Test Run, the hadronic running will be detected just as a linear deviation in t on the shape of R_{had}. It follows that the template fit will be performed to find only the parameter K in the Test Run. The resulting value of a template fit to the ratio R_{had} is $K = 0.136 \pm 0.026$.

4. – Conclusions and future plans

The MUonE experiment could provide an independent evaluation of a_μ^{HLO}, competitive with the latest evaluations, and could help to understand the current muon g-2 puzzle.

Intense activity is ongoing for the preparation of the Test Run, which will be a proof of concept of the overall project. If successful, a full proposal will be prepared, including support from the results of the Test Run. The full detector construction will then take place during the LHC Run3, with the aim of performing a first measurement of a_μ^{HLO} before the Long Shutdown 3 foreseen in 2026–28.

REFERENCES

[1] Muon g-2 Collaboration (Abi B. *et al.*), *Phys. Rev. Lett.*, **126** (2021) 141801.
[2] Muon g-2 Collaboration (Bennett G. W. *et al.*), *Phys. Rev. D*, **73** (2006) 072003.
[3] Aoyama T. *et al.*, *Phys. Rep.*, **887** (2020) 1.
[4] Muon g-2 Collaboration (Grange J. *et al.*), *Muon (g-2) Technical Design Report* (2015) `https://arxiv.org/abs/1501.06858`.
[5] Abe M. *et al.*, *Prog. Theor. Exp. Phys.*, **2019** (2019) 053C02.
[6] Jegerlehner F and Nyffeler A., *Phys. Rep.*, **477** (2009) 1.
[7] Borsanyi S. *et al.*, *Nature*, **593** (2021) 51.
[8] Carloni Calame C. M., Passera M., Trentadue L. and Venanzoni G., *Phys. Lett. B*, **746** (2015) 325.
[9] Lautrup B. E., Peterman A. and de Rafael E., *Phys. Rep.*, **3** (1972) 193.
[10] Abbiendi G. *et al.*, *Eur. Phys. J. C*, **77** (2017) 139.
[11] MUonE Collaboration (Abbiendi G. *et al.*), *Letter of Intent: the MUonE project*, CERN-SPSC-2019-026/SPSC-I-252 (2019).
[12] Abbiendi G. *et al.*, *JINST*, **15** (2020) P01017.
[13] Alacevich M. *et al.*, *JHEP*, **02** (2019) 155.
[14] Fael M., *JHEP*, **02** (2019) 027.
[15] Fael M. and Passera M., *Phys. Rev. Lett.*, **122** (2019) 192001.
[16] Mastrolia P., Passera M., Primo A. and Schubert U., *JHEP*, **11** (2017) 198.
[17] Di Vita S. *et al.*, *JHEP*, **09** (2018) 016.
[18] Di Vita S. *et al.*, *JHEP*, **06** (2019) 117.

[19] Bonciani R. *et al.*, *Phys. Rev. Lett.*, **128** (2022) 022002.
[20] Carloni Calame C. M. *et al.*, *JHEP*, **11** (2020) 028.
[21] Banerjee P., Engel T., Signer A. and Ulrich Y., *SciPost Phys.*, **9** (2020) 027.
[22] Budassi E. *et al.*, *JHEP*, **11** (2021) 098.
[23] Fael M., Lange F., Schoenwald K. and Steinhauser M., *Massive vector form factors to three loops* (2022) https://arxiv.org/abs/2202.05276.
[24] Balzani E., Laporta S. and Passera M., arXiv:2112.05704 [hep-ph] (2022).
[25] Banerjee P. *et al.*, *Eur. Phys. J. C*, **80** (2020) 591.
[26] Masiero A., Paradisi P. and Passera M., *Phys. Rev. D*, **102** (2020) 075013.
[27] Dev P. B., Rodejohann W., Xu X. J. and Zhang Y., *JHEP*, **05** (2020) 053.
[28] CMS Collaboration, *The Phase-2 Upgrade of the CMS Tracker*, CERN-LHCC-2017-009/CMS-TDR-014 (2017).
[29] Rose A. *et al.*, *PoS*, **TWEPP2018** (2019) 115.